Deuterium thermal desorption from FeAl thin films

2002 J. Phys.: Condens. Matter 14 6307

(http://iopscience.iop.org/0953-8984/14/25/301)

INSTITUTE OF PHYSICS PUBLISHING JOURNAL OF PHYSICS: CONDENSED MATTER

J. Phys.: Condens. Matter **14** (2002) 6307–6320 PII: S0953-8984(02)32264-1

Deuterium thermal desorption from FeAl thin films

R Checchetto[1,4], A Miotello[1], C Tosello[1], G Principi[2] and P Mengucci[3]

[1] Istituto Nazionale per la Fisica della Materia (INFM), Dipartimento di Fisica dell'Università di Trento, I-38050 Povo (TN), Italy
[2] Istituto Nazionale per la Fisica della Materia (INFM), Dipartimento di Ingegneria Meccanica e Strutturale dell'Università di Padova, I-35131 Padova, Italy
[3] Istituto Nazionale per la Fisica della Materia (INFM), Dipartimento di Fisica e Ingegneria dei Materiali e del Territorio dell'Università di Ancona, I-60131 Ancona, Italy

E-mail: checchet@science.unitn.it

Received 3 January 2002, in final form 26 March 2002
Published 14 June 2002
Online at stacks.iop.org/JPhysCM/14/6307

Abstract

Deuterium thermal desorption experiments were performed on B2 FeAl thin films deposited by electron-beam evaporation on Si substrates, annealed at temperatures ranging from 673 to 773 K and implanted with 20 keV D_2 ions at fluences of 3×10^{16} D_2^+ cm^{-2}. D_2 desorption spectra, recorded in isochronal heating conditions (0.5 K s^{-1} temperature ramp), show two well resolved desorption peaks at ∼500 and 820 K. The first peak is attributed to the desorption of deuterium contained in FeAl weakly bonding sites of the FeAl lattice, probably point defects (vacancies) produced by the ion implantation process. The second peak is attributed to deuterium release from trapping sites in the FeAl lattice that could be the defect complexes formed by the association of a vacancy in the Fe sublattice and a substitutional Fe atom in the Al sublattice (V_{Fe}–Fe_{Al}).

The desorption kinetics can be reproduced by assuming that:

(a) deuterium desorption at ∼500 K is controlled by the D_2 surface recombination process with $E_{des} = 1.57 \pm 0.02$ eV as activation energy;
(b) deuterium desorption at ∼820 K is controlled by the release of D atoms from the trap sites, a process which occurs in connection with defect relaxation.

The energy of interaction of deuterium with this trapping site can be estimated to be ∼2 eV.

1. Introduction

Ordered intermetallic compounds based on iron aluminides belong to a class of structural materials important because of their excellent oxidation and corrosion resistance: in fact,

[4] Author to whom any correspondence should be addressed.

when the Al concentration in the alloy is larger than ∼10 wt% a continuous fully adherent alumina layer forms on the surface [1]. The most interesting Fe–Al equilibrium phases are:

(a) the disordered α-Fe (Al) bcc solid solution with Al atoms dissolved up to 45 at.%,

(b) the FeAl (B2) phase with about 36–48 at.% Al and cubic CsCl structure, that forms through ordering of the α-Fe and is stable at room temperature, and

(c) the Fe_3Al (DO3) phase with cubic BiF_3 structure, that forms through a second-order phase transition from FeAl and is stable in the 23–36 at.% Al range [2].

During the last few decades many efforts have focused on enhancing the room temperature ductility, the high-temperature strength, and the high-temperature creep resistance of this intermetallic compound to stimulate applications as high-temperature structural material [3].

According to theoretical studies and experimental analysis [4, 5], vacancies are the predominant point defects in the stoichiometric FeAl B2-type lattice. Conversion electron Mössbauer spectroscopy (CEMS) analysis [5] has shown that these defects are mostly formed on the Fe sublattice (V_{Fe}) together with a high concentration of antisite Fe atoms (Fe_{Al}). Many investigations have shown a strong connection between vacancy concentration and mechanical properties of iron-based aluminides: two remarkable examples are the strong dependence of the FeAl hardness on the cooling rate, proving a role as regards the quenched-in vacancies [6,7], and the linear dependence of the alloy yield strength increase on the square root of the vacancy concentration [8].

The poor ductility of FeAl and Fe_3Al at room temperature is attributed to the susceptibility of this material to hydrogen embrittlement (HE): atomic hydrogen is supposed to be created in the interaction of Al atoms in the surface with water vapour present in the atmosphere, as described by the reaction

$$2Al_{(surf)} + 3H_2O_{(gas)} \rightarrow Al_2O_{3(surf)} + 6H_{(abs)}.$$

Evidence of this is provided by significant improvement of tensile elongations of FeAl when tested either in vacuum or oxygen atmosphere [9]. Only poor information is available on the interaction between hydrogen and point defects in the intermetallic FeAl bcc phase and it is mainly connected with the analysis of the hydrogen diffusion at ambient temperature. Banerjee and Balasubramaniam [10] evidenced that an increase in the amount of Al in the Fe–Al alloy lowers the hydrogen diffusivity at room temperature, which can be further reduced by alloying the material with Cr and Ti because of the trapping ability of these elements. Yang and Hanada [11] measured the hydrogen diffusivity in ordered B2 Fe–40Al alloys and observed H diffusivity during absorption higher than that during desorption.

In this paper we will present an experimental study on the thermal desorption process of deuterium ions implanted in stoichiometric FeAl thin films having B2-type crystalline structure. Two deuterium desorption peaks were observed at temperatures of ∼500 and 820 K. Deuterium desorbing at low temperature is weakly bonded to the B2 lattice: a comparison with literature data on hydrogen in metals indicates that the site where it is contained is a free interstitial site or a vacancy in the host B2 lattice. Deuterium desorbing at temperatures close to 820 K is strongly bonded with the host lattice, suggesting the presence of a D-trapping process: we suggest that the trapping centre is related to the defect complex formed by the association of a vacancy in the Fe sublattice and a substitutional Fe atom in the Al sublattice of the FeAl B2 structure (V_{Fe}–Fe_{Al}).

The results obtained suggest that the presence of homogeneously distributed deep trapping sites in the FeAl lattice, by limiting the diffusivity of hydrogen isotopes, can reduce HE effects.

2. Experimental details

The samples were prepared starting with a Fe–Al multilayer deposited on (100)-oriented Si wafers by sequential evaporation of 15 couples of 10 nm Fe and 14 nm Al layers in an UHV chamber having residual vacuum in the low 10^{-7}–10^{-6} Pa range: given the atomic densities of 0.85×10^{23} and 0.6×10^{23} atoms cm^{-3} for Fe and Al, respectively, the thickness of each metallic layer was chosen to ensure an average 1:1 atomic composition of the deposited sample. To enhance the atomic mixing and promote the formation of the intermetallic FeAl B2 phase, the samples were transferred to an UHV heating chamber and subjected to thermal annealing at temperatures ranging from 673 to 773 K [12]. Some samples were also annealed in air to promote the formation of a surface oxide layer.

All the samples were implanted at room temperature by using 20 keV D_2 ions at 3×10^{16} D_2^+ cm^{-2} fluence. The film thickness was established after TRIM simulations [13] in order to have all the implanted ions inside the deposited film: the medium projected range, R_P, of the ions is ∼160 nm and the longitudinal straggling, ΔR_P, is ∼40 nm.

Thermal desorption spectroscopy (TDS) analyses were performed in an UHV stainless steel chamber equipped with a quadrupole mass spectrometer (QMS) [14]. The experiments were carried out by heating the sample with a linear ramp of 0.5 K s^{-1} up to ∼1200 K and measuring the QMS D_2^+ mass signal ($m/e = 4$): at constant pumping speed of the vacuum apparatus, the QMS signal is directly proportional to the value of the deuterium desorption rate. Experimental errors in the deuterium desorption signal were estimated from the mean value of the fluctuations in the $m/e = 4$ background signal.

The local environment of Fe atoms in the samples was studied by CEMS: the spectra were recorded at room temperature by using a conventional spectrometer with a flowing-gas proportional counter and a source of ^{57}Co of about 10 mCi activity in a Rh matrix. A standard least-squares-minimization routine was used to fit the spectra profiles as a superposition of Lorentzian lines. Rutherford backscattering spectroscopy analysis was performed by using a 2.0 MeV $^4He^+$ beam to study the composition of the surface oxide after thermal annealing of the samples in air: measurements were performed with the α-particle beam normal to the surface and the detector placed at a 100° scattering angle. Information on the crystal structure of the film and of the surface oxide layer were obtained by glancing-angle x-ray diffraction (GAXRD) by using an INEL diffractometer equipped with a CPS 120 curved detector.

3. Results

In figures 1 and 2 we present XRD and CEMS spectra of the Fe–Al multilayer samples subjected to thermal annealing in UHV conditions at a temperature of 773 K for 80 h. As observed in a previous paper [12], this thermal treatment induces the complete mixing of the multilayer sample and the formation of a defective B2-type FeAl phase. The XRD spectrum of figure 1 displays the peaks characteristic of the B2 FeAl structure, indicating a strong preferred orientation in the (110) direction with estimated grain size larger than 50 nm. The CEMS spectrum in figure 2 can be well fitted assuming that ∼83% of the Fe atoms are in ordered B2 FeAl positions (dotted curve), ∼2% in antisite positions of the FeAl B2 phase (dashed curve), and ∼15% in corner antisite positions of the FeAl B2 phase (dash–dotted curve) [12]. The desorption spectrum of a deuterium-implanted sample is shown in figure 3: we observe a structured spectrum presenting a strong desorption peak at ∼500 K and a well resolved second peak at ∼820 K. In the spectrum, experimental data are presented as open symbols along with experimental errors, while the solid curve is the best-fit result as obtained by numerical solution of desorption equations (see the next section).

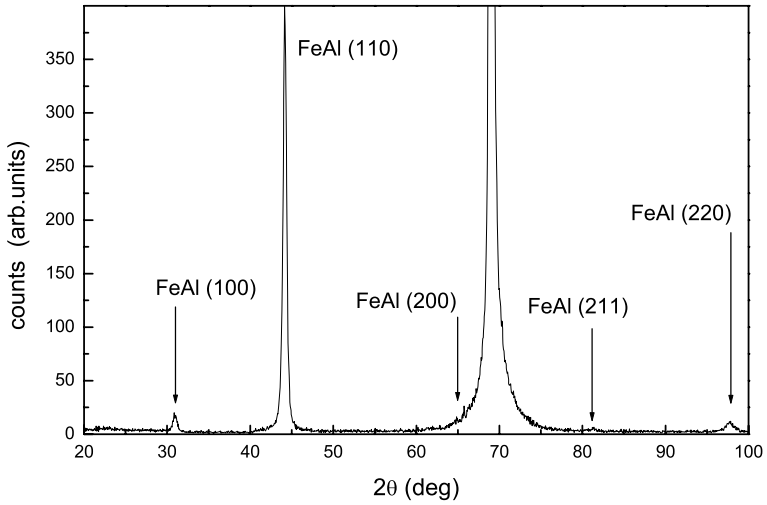

Figure 1. The XRD diffraction pattern of the Fe–Al multilayer sample subjected to thermal annealing in UHV at 773 K for 80 h. The strong peak at $\sim 70^{\circ}$ is related to the Si substrate.

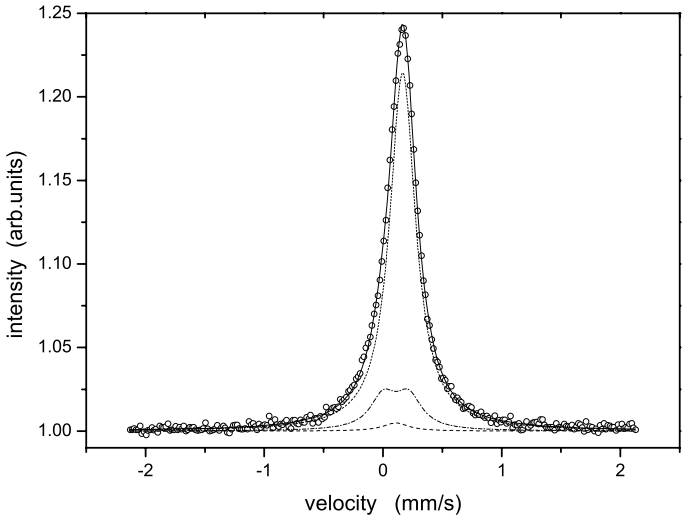

Figure 2. The Mössbauer spectrum of the Fe–Al multilayer sample subjected to thermal annealing in UHV at 773 K for 80 h. Key: open circles: data points; continuous thick curve: best fit; short-dashed curve: Fe atoms in ordered Be FeAl; dash–dotted curve: Fe atoms in antisite positions; dashed curve: Fe atoms in corner antisite positions.

To prepare the oxidized sample, we subjected a Fe–Al multilayer treated in UHV conditions (873 K thermal annealing for 240 min) to thermal annealing in air at 873 K for 240 min. In figures 4(a) and (b) we present the RBS profiles of the oxidized sample and, for comparison, of an UHV-annealed sample which was not subjected to treatment in air. We observe the presence of an oxide layer $\sim$1 nm thick. No diffraction peaks pertinent to an oxide phase were observed in the XRD spectrum even at glancing-angle incidence; see figure 5. No Fe–O signals were revealed by CEMS analysis (not reported here). We thus conclude that the oxide layer grown on the surface of the B2 FeAl thin film can be attributed to

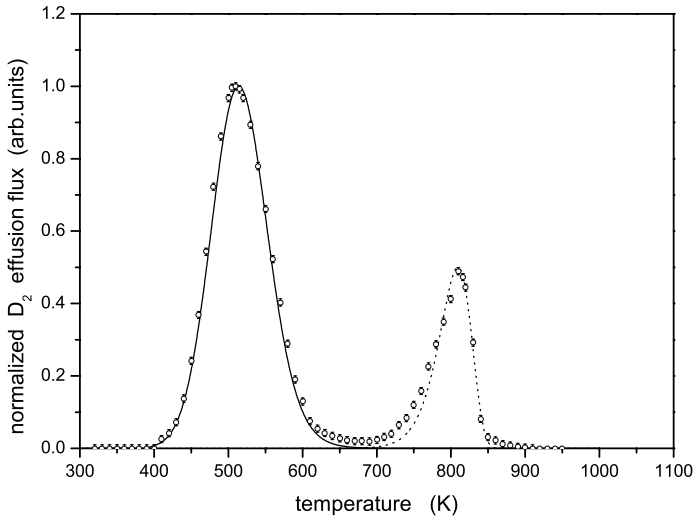

Figure 3. The deuterium TDS spectrum of the FeAl thin film of figures 1 and 2. Symbols: experimental data. Line: simulation (see the text).

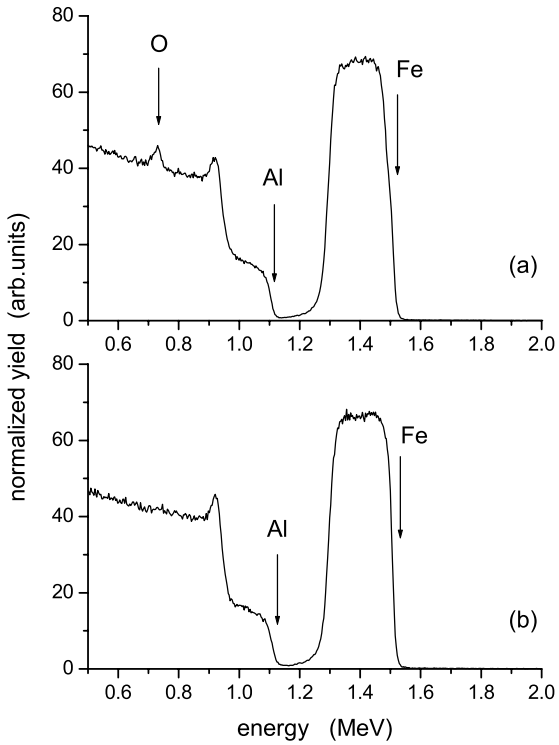

Figure 4. (a) The RBS spectrum of the FeAl thin film subjected to thermal annealing in air to promote the formation of a surface oxide layer. (b) The RBS spectrum of the sample prior to the oxidation process.

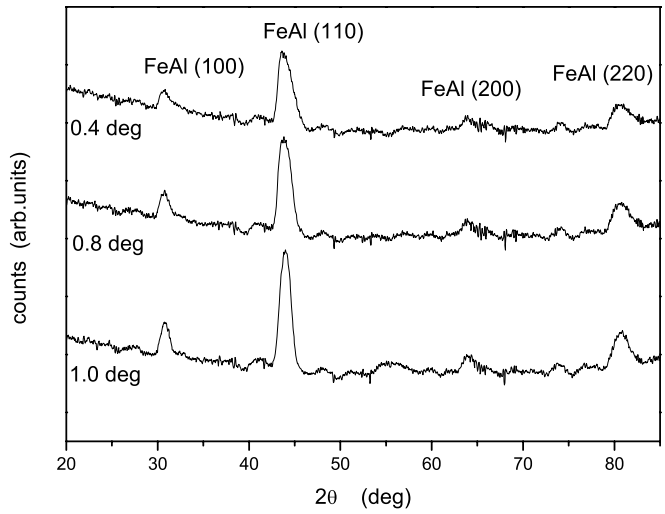

Figure 5. Glancing-angle XRD diffraction patterns of the FeAl thin film subjected to thermal annealing in air to promote the formation of a surface oxide layer.

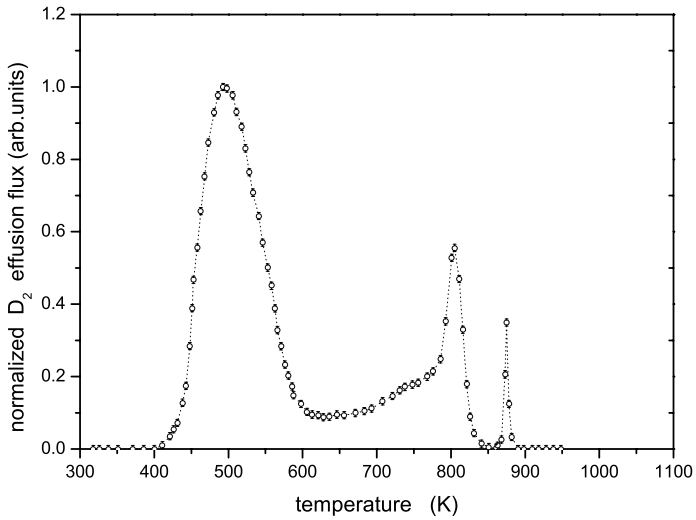

Figure 6. The deuterium TDS spectrum of the oxidized FeAl thin film of figures 4(a) and 5. The curve in the figure is only a guide for the eye.

a thin Al oxide layer with an amorphous structure. These indications are in agreement with an experimental study of Graupner *et al* [15] on the surface oxidation of B2-type FeAl samples: the authors observed, in fact, that in the oxidation of low-index FeAl surfaces there was no interaction of oxygen with Fe atoms and that the grown oxide was approximately 0.5 nm thick.

The desorption spectrum of deuterium implanted in the oxidized sample is presented in figure 6: in the spectrum we observe the desorption peak at 500 K, the desorption peak at 820 K with a shoulder on the low-temperature side, and a new well resolved desorption peak at 870 K.

4. Discussion

A simple model for analysing deuterium desorption considers the kinetics as given by the cooperation of three processes:

(a) release of deuterium atoms from the solution sites where they are contained (interstitial sites or weakly bonded states),
(b) atomic diffusion to the sample surface, and
(c) recombinative desorption of the D atoms from the surface to the gas phase.

Hydrogen diffusion in metals is a very fast process: the time τ_{diff} needed by D atoms to travel along the film thickness d can be estimated from the random walk expression: $\tau_{diff} = d^2/D_{diff}$, where D_{diff} is the diffusion constant of hydrogen in FeAl. With $D_{diff} \sim 10^{-5}$ cm^2 s^{-1} at 500 K in iron-based intermetallic materials [16], we estimate a value of 10^{-3} s for τ_{diff}. The characteristic time for deuterium desorption T_p/α (in this expression T_p is the peak temperature and α the heating ramp) is, in the present experiment, much larger than τ_{diff}, being $\sim 10^2$ s for the peak at $\sim$500 K and $\sim 10^3$ s for the peak at $\sim$820 K. We, hence, neglect the diffusion process in the analysis of our results because it occurs on a timescale quite a lot smaller than that of our experimental data.

When the desorption kinetics can be described as a thermally activated process having a defined activation energy E_0, the desorption rate $r(t)$ is given by [17]

$$r(t) = -\frac{\mathrm{d}C}{\mathrm{d}t} = -\frac{C^n}{\tau(T_0, E_0)} \tag{1}$$

where $\tau(T, E_0) = \tau_0 \exp(E_0/k_B T)$ is a characteristic time, a function of the sample temperature T (in our experiment $T = T_0 + \alpha t$, α is the temperature ramp), and $\tau_0 \sim 10^{-13}$ s; n is the order of the reaction. If C_0 is the total amount of deuterium involved in the desorption process, the solution of equation (1), with initial condition $C(0) = C_0$, is given by

$$C(t) = C_0 \exp\left(-\frac{t}{\tau(T, E_0)}\right) \tag{2}$$

and the desorption rate $r(t)$ can be calculated as

$$r(t) = -\frac{\mathrm{d}C}{\mathrm{d}t} = \frac{C_0}{\tau} \exp\left(-\frac{t}{\tau}\right). \tag{3}$$

When the process presents heterogeneity in the activation energy values, the solution of equation (1) can be obtained by weighting the contribution of each site, having activation energy E, to the desorption flux $r(t)$ with its own probability:

$$C_h(t) = \int_0^\infty C(t, E)\varphi(E)\,\mathrm{d}E \tag{4}$$

where $\varphi(E)\,\mathrm{d}E$ represents the fraction of deuterium that desorbs with activation energy values between E and $E + \mathrm{d}E$ with the normalization condition [18]

$$\int_0^\infty \varphi(E)\,\mathrm{d}E = 1.$$

In figure 3 we show the deconvoluted peaks and the total desorption rate which are in the best agreement with the experimental data. The best fit of the desorption peak at $\sim$500 K was obtained with a second-order kinetics and assuming for the activation energy a Gaussian distribution:

$$\varphi_{E_0,\sigma}(E) = \frac{1}{\sigma\sqrt{2\pi}} \exp\left(-\frac{(E - E_0)^2}{2\sigma^2}\right),$$

where $E_0 = 1.57 \pm 0.02$ eV and $\sigma = 0.10 \pm 0.01$ eV.

The best fit of the desorption peak at ∼820 K was obtained with a homogeneous first-order kinetics where $E_0 = 2.56 \pm 0.02$ eV.

Let us analyse the low-temperature D_2 desorption peak. Second-order desorption processes have been observed very often in studies of the release of light atoms forming diatomic molecules from solution in metals. This kind of process was generally interpreted as indicating the recombinative desorption of gas atoms at the metal surface as the rate-limiting mechanism [19]:

$$2D_{surf} \rightarrow D_{2(gas)}.$$

The measured value of 1.57 ± 0.02 for E_{des} can be compared with the energy barrier value for D_2 desorption pertinent to pure Fe and Al surfaces. From TDS measurements, Boszo *et al* [20] observed that deuterium desorption from Fe surfaces was a second-order process, thus indicating the D_2 surface recombination as the limiting process. In the case of nearly complete coverage, the authors measured activation energy values (E_{des}) ranging from 0.9 to 1.1 eV depending on the crystallographic orientation of the Fe surface. The desorption of deuterium from the Al surface is a quite different process. Mundenar *et al* [21] exposed the Al(111) surface to atomic hydrogen at 100 K and observed that the D_2 desorption occurred at 350 K following a zero-order kinetics with $E_{des} = 0.7 \pm 0.1$ eV. The observed kinetics suggested that desorption was controlled by the release of D atoms from surface defects. Theoretical calculations predicted, in fact, an activation energy E of only 0.5 eV for the recombinative H_2 desorption from the Al(111) surface [21].

The value of E_{des} resulting from the present experiment seems quite reasonable if we assume that deuterium atoms in the FeAl surface interact strongly with the transition metal component of the aluminide. This idea is confirmed by an experimental study of Gleason *et al* [22] on the chemistry of water on polycrystalline TiAl, FeAl, and NiAl intermetallic compounds: in fact the authors observed that TDS spectra of hydrogen resulting from the decomposition of water in the aluminide surfaces are similar to the TDS spectra obtained from the corresponding transition metal. It is worth noting that this idea is in line with the embrittlement mechanism suggested by McKamey *et al* [9].

When H atoms are contained in surface chemisorption sites, the activation energy for desorption depends not only on the composition of the surface but also on its structure and cleanliness. The FeAl thin-film samples used in our experiments are strongly oriented, as indicated by the dominant FeAl(110) XRD reflection in figure 1. The measured value of 1.57 ± 0.02 eV represents thus the activation energy of D_2 desorption from the FeAl(110) plane. In general we should expect different values of the energy barrier for desorption in different plane orientations, as shown by Boszo *et al* in Fe [20] and Brzóka and Kleint in Si [23]. In has not been possible to test this point, because our FeAl samples with good crystallinity always present the strong (110) orientation. The presence of contaminants on the sample surface can also influence the value of the activation energy for desorption. In many metals it has been observed that CO adsorption, for example, produces H desorption peaks at temperatures lower than for the clean metal surface, indicating that coadsorbed carbon monoxide weakens the metal–H binding energy [24–26]. However, we suggest that coadsorbed impurity does not influence the deuterium desorption kinetics, as observed in the present experiments: instead the observed D_2 desorption peaks from FeAl occur at quite high temperatures, ∼500 and 820 K, well beyond the temperature interval where adsorbed contaminants are degassed [27].

The best fit of the high-temperature D_2 desorption peak in figure 3 was obtained assuming that the deuterium release obeys a first-order kinetics occurring as a consequence of deuterium detrapping. Before going on with the discussion, it is important to remark that in the present experiment the bonded state of deuterium, and thus the observed first-order kinetics, cannot be

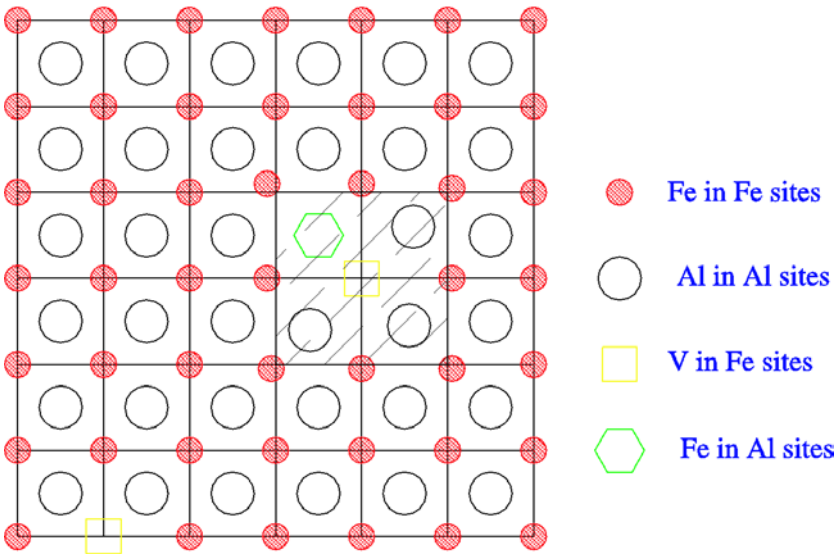

Figure 7. A schematic diagram of the B2-phase FeAl and the local environments of point defects. The dashed zone indicates the V_{Fe}–Fe_{Al} defect complex.
(This figure is in colour only in the electronic version)

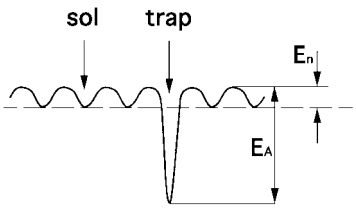

Figure 8. Energy levels of solution sites ('*sol*') and trapping sites ('*trap*') where hydrogen resides in the metal host. E_A: activation energy needed by a D atom to escape from a trapping centre; E_n: activation energy needed to leave a normal solution site.

explained by the formation of any hydride phase [28] because neither Fe nor Al forms stable hydrides [29]. In the rest of the discussion we will thus consider the trapped state of deuterium as due to interaction with crystalline defects of the host atomic lattice.

In figure 8 we show the energy levels of solution sites ('*sol*') and trapping sites ('*trap*') where deuterium resides in the host metal. The activation energy E_A needed by a D atom to escape from a trapping centre is much higher than the energy needed to leave a normal solution site, E_n. E_A is given by the sum of the trap–deuterium interaction energy, E_{trap}, and the activation energy for deuterium diffusion in the normal lattice, E_n.

To obtain an estimate of the energy term E_{trap}, we can refer to the current literature on hydrogen diffusion through Fe base aluminides. Chen and Wan [30] carried out tests of hydrogen permeation through Fe_3Al intermetallic by a double-cell electrochemical method and measured an E_n-value of ∼0.4 eV in the 285–330 K temperature interval. Schwendemann and Kronmueller [31] studied the relaxation behaviour of hydrogen in Fe-based aluminides by means of magnetic after-effect measurements and observed activation energies of 0.13 and 0.35 eV for the relaxation maxima. The relaxation processes were attributed to the jumps of

H isotopes between two energetically different interstitial configurations. This information indicates that the major contribution to the E_A-values arises from the E_{trap}-term, which can be evaluated to be ∼2 eV.

This binding energy is large and quite different from the typical values for deuterium bonding to the defects created in a metal under ion implantation: vacancies, interstitials, and extended defects [32]. Binding energies of H with vacancies in metals (expressed relative to H in solution) exhibit, for example, values of 0.52 eV for Al [33] and 0.63 eV for Fe [34]: these binding energies tend to be comparable to those of H atoms in chemisorption sites because the local open volume associated with the vacancy appears to an H atom as a free surface. Binding energies of H with solute in metals take values close to 0.1 eV—for example, for Fe substitutionals in Ni: 0.07–0.12 eV [35] and for C in Fe: 0.03 eV [36]. The binding to interstitial atoms depends on the lattice distortion near the interstitial site and on the consequent reduced host-atom density: the binding is thus expected to be weaker than at the vacancy. For fully metallic grain boundaries, the binding with internal boundaries in metals presents comparable energy values—for example, 0.15 eV for Al [37] and 0.17–0.48 eV for Pd [38]. These values indicate the absence of open-volume regions in extended defects of this kind.

The estimated value of $E_{trap} \sim 2$ eV, for metals, generally indicates the occurrence of chemical bonding for deuterium. Myers and Follstaedt [39], for example, studied the trapping of deuterium in Al samples presenting γ-Al_2O_3 surface precipitates as a consequence of O-ion implantation. By ion-beam analysis, the authors evaluated a deuterium-trapping energy of 0.7 eV relative to D in solution, which was attributed to the formation of molecular D_2 at the Al_2O_3–Al boundary, and trapping energy above 1 eV, evidencing the formation of chemical bonds of deuterium atoms at oxide defects. Similar values have also been measured for hydrogen trapping with internal boundaries in metals involving non-metal species, as in the case of the Al_2O_3–Pd boundary in Pd, 0.9 eV [40], and ∼1 eV for TiC–Fe boundaries in Fe [41], presumably indicating the formation of partially covalent bonding.

To test this possibility, we implanted deuterium in FeAl thin-film samples having an intentionally grown surface oxide layer; see figures 4(a), (b) and figure 5. Although minor differences can be observed, if we compare the TDS spectrum in figure 3 pertinent to the non-oxidized sample and the TDS spectrum of the oxidized sample presented in figure 6, we observe that the most important difference in the deuterium desorption signal is a very narrow desorption peak at ∼870 K. This peak is well resolved from the peak at ∼820 K present in the TDS spectrum of the non-oxidized sample, indicating that in the deuterium desorption kinetics presented in figure 3 the surface oxide layer does not play an important role.

The comparison of the evaluated value for E_{trap} with literature data thus indicates that the typical defects, produced during deuterium-ion implantation, cannot be responsible for the large value of the trapping energy evaluated in the present work. The evolution of deuterium at high temperature is controlled by a more complex kinetics involving not only the deuterium release from the sites where it is accommodated in the host lattice, but also the evolution of the defect microstructure.

Point defects in stoichiometric and well annealed B2-phase FeAl samples were studied by Bogner *et al* [42] by using ^{57}Fe Mössbauer spectroscopy. The authors observed that the Mössbauer spectra of stoichiometric samples were reproduced assuming only the presence of Fe_{Al} antisite and V_{Fe} vacancy defects: in stoichiometric crystal—see figure 7—each Fe_{Al} antisite atom is compensated by two V_{Fe} vacancies. An indication of the role of these defects in the control of the deuterium desorption kinetics is given by a recent paper of Schaefer *et al* [43]: in internal friction studies (mechanical spectroscopy) the authors observed the presence of atomic defects producing an internal friction maximum at 680 K which was ascribed to the reorientation of V_{Fe}–Fe_{Al} complexes. The observed thermal reorientation of the complex

occurs just before the onset of the deuterium desorption peak at a temperature of ∼820 K. We tentatively suggest that trapped deuterium is contained in the V_{Fe}–Fe_{Al} complex and that the detrapping from these defects occurs after the orientational relaxation of the defect: after detrapping, deuterium immediately desorbs from the sample surface, because at temperatures of ∼820 K, surface processes are already activated.

Except for the coincidence between defect relaxation and deuterium desorption, we do not have direct evidence of D trapping by V_{Fe}–Fe_{Al} complexes: we can only discuss the plausibility of this attribution on the basis of literature data on different metal–hydrogen systems. A strong trap for implanted hydrogen was observed by Myers *et al* [44] in Y-implanted Fe: by an ion-beam technique, the authors observed the presence of deuterium traps with 1.3 eV binding energy. The authors indicated as the trapping centre a defect complex stabilized by the oversized Y atom. The oversized Y atom in the Fe host lattice (the atomic radius of Y is 1.41 times that of Fe) produces a strong lattice perturbation attracting vacancies and finally resulting in a Y–vacancy complex which strongly binds hydrogen. It is reasonable to assume that the process is only controlled by vacancies produced by the ion implantation process because, for the present implantation energy, 20 keV, and fluence, 6×10^{16} D^+ cm^{-2}, vacancies are produced in excess of one per D atom.

It is of interest to consider whether the V_{Fe}–Fe_{Al} defect complex forms immediately after implantation or during the TDS heating procedure. We suggest that, as deuterium atoms are mobile at room temperature [16], they would immediately be trapped by these complex defects if they were present in the as-implanted sample. However, TDS spectra indicate that the majority of the implanted deuterium is released at low temperature (∼500 K) from free interstitial sites: we can thus argue that the formation of the defect complex, strongly trapping deuterium, is a delayed process. This idea is plausible, considering that V_{Fe} has a very low diffusivity in the FeAl B2 phase as evidenced by the high diffusion enthalpy measured by Würschum *et al* in a study by positron annihilation spectroscopy (PAS) [45]: the authors measured, in fact, a rather high value of 1.7 eV.

We thus suggest the following three-step model to describe the microscopical state of deuterium implanted in FeAl B2-phase thin films:

(i) as-implanted deuterium is contained in weakly bonded states related to the host lattice, probably vacancies produced by the ion implantation process in the B2 FeAl lattice;
(ii) during the TDS temperature ramp the majority of the implanted deuterium effuses from the sample but a fraction is trapped by the V_{Fe}–Fe_{Al} defect complexes; their formation does not require, in fact, long-range mobility of the vacancy;
(iii) the release of deuterium from the V_{Fe}–Fe_{Al} complex occurs in connection with the defect orientational relaxation.

The third step in the proposed model was observed by the present authors also in a different systems [46, 47]. High-purity synthetic quartz contains, as the typical impurity, Al^{3+} ions substituting for Si^{4+}. When quartz is subjected to the 'air-sweeping' process [48], alkali metal ions, which compensate in the material for the charge deficiency of the Al^{3+} ion, are replaced by protons (from H_2O vapour in air) producing Al–OH defect centres. We observed by TDS spectroscopy that in air-swept samples, hydrogen re-emission occurred simultaneously with the dissociation of the Al-related defect centres, as indicated by differential scanning calorimetry (DSC) analysis [46, 47].

It is important to analyse also the possible role of vacancy clusters in the control of the deuterium release. Clustering of vacancies in metals produces microvoids and, in metals having low hydrogen solubility, the capture of deuterium from solution produces bubbles: we exclude this trapping mechanism from consideration, because the formation of large voids would

require long-range mobility of the vacancies. Scanning electron microscopy (SEM) analysis, in fact, does not indicate the presence of bubbles at the surface of our FeAl samples [49].

Before concluding this discussion, it is important to point out that the process of diffusion of Si atoms from the substrate to the FeAl layers could explain the deuterium release at high temperature. Bayer and Wagner [50] observed in sputter-deposited a-Si:H thin films hydrogen desorption at a temperature of ∼600 °C, which was associated with the release of single H atoms from isolated and strongly bonding ≡SiH and =SiH_2 centres. The Si–H binding energy is quite large, approximately 3 eV [51], but the effective value of the activation energy for H desorption turned out to be lower because it involved the energy gain due to the formation of Si–Si bonds after H release. During the high-temperature thermal annealing of the FeAl thin-film samples in the TDS experiment, Si atoms of the substrate may become mobile, and penetrate the FeAl lattice and form Si–D bonds in the interaction with implanted D atoms. Let us suppose that this process is operative in our samples. In figure 3 we observe that about a third of the implanted D atoms are released at high temperature ($T > 800$ K). In the present 300 nm thick samples the implantation fluence was 3×10^{16} D_2 cm^{-2}: this would imply a concentration of Si atoms forming Si–D bonds close to 10^{21} Si cm^{-3}. We think that so large a Si content would have involved not only Si–D chemical bonds, but also the formation of Fe–Si phases.

The XRD and CEMS analyses performed on the FeAl samples do not show evidence of iron silicide formation. All the diffraction peaks observed in the XRD spectrum of figure 1 are, in fact, pertinent to the B2 FeAl phase. Let us consider now the CEMS spectra in figure 2: the doublet which we have attributed to Fe atoms in defect positions presents fitting parameters which are quite close to that of the iron silicide [52]. If this doublet were due to the formation of Fe silicide after diffusion of Si atoms from the substrate to the FeAl layers, its intensity would increase on increasing the temperature and duration of the annealing treatment. However, we observe the reduction of this doublet [12]: this evidence is compatible with the reduction of structural defects in the thermally treated samples.

5. Conclusions

In B2-phase FeAl thin films, ion-implanted deuterium is contained in weakly bonded sites of the host atomic lattice. Thermal treatment during the TDS run induces the formation of complex defects which can strongly trap a fraction of the implanted deuterium. The TDS spectra of deuterium-implanted FeAl thin film consequently show a low-temperature desorption peak at ∼500 K and a second high-temperature peak at a temperature of ∼820 K.

The desorption kinetics can be reproduced by assuming that:

(a) deuterium desorption at ∼500 K is controlled by the D_2 surface recombination process with $E_{des} = 1.57 \pm 0.02$ eV as the activation energy;
(b) deuterium desorption at ∼820 K is controlled by the release of D atoms from the trap sites, a process which occurs in connection with defect relaxation.

This defect is tentatively suggested to be in the complex formed by the association of a vacancy in the Fe B2 sublattice and a neighbouring Fe atom in the Al sublattice (V_{Fe}–Fe_{Al}), and the energy of interaction of deuterium with this trapping site is estimated to be ∼2 eV.

Acknowledgments

We are very grateful to R Tonini, Dipartimento di Fisica dell'Università di Modena, for the deuterium-ion implantation.

This work received specific financial support from the Ministero Istruzione Università e Ricerca (MIUR, COFIN 2001) and the Istituto Nazionale per la Fisica della Materia (INFM).

References

[1] Sauthoff G 1990 *High Temperature Aluminides and Intermetallics* ed S H Whang, C T Liu, D P Pope and J O Stiegler (Warrendale, PA: Minerals, Metals and Materials Society) p 329
[2] Kattner U R 1990 *Binary Alloy Phase Diagrams* ed T B Massalski (Metals Park, OH: ASM International) p 147
[3] Deevi S C and Sikka V K 1996 *Intermetallics* **4** 357
[4] Fu C L, Ye Y Y, Yoo M H and Ho K M 1993 *Phys. Rev.* B **48** 6712
[5] Collins G S and Peng L S J 1996 *Nuovo Cimento* **18** 329
[6] Lui C T, Lee E H and McKamey C G 1989 *Scr. Metall.* **23** 875
[7] Napgal P and Baker I 1990 *Metall. Trans.* A **22** 2281
[8] Baker I and George E P 1998 *Phil. Mag.* A **77** 737
[9] McKamey C G, Horton J A and Liu C T 1988 *Scr. Metall.* **22** 1679
[10] Banerjee P and Balasubramaniam R 1998 *Scr. Mater.* **39** 1215
[11] Yang Y and Hanada S 1995 *Scr. Metall. Mater.* **32** 1719
[12] Checchetto R, Tosello C, Miotello A and Principi G 2001 *J. Phys.: Condens. Matter* **13** 811
[13] Ziegler J F, Biersack J P and Littman U 1985 *The Stopping and Range of Ions in Solids* (New York: Pergamon)
[14] Checchetto R, Gratton L M, Miotello A and Cestari C 1995 *Meas. Sci. Technol.* **6** 1605
[15] Graupner H, Hammer L, Heinz K and Zehner D M 1997 *Surf. Sci.* **380** 335
[16] Yang L and McLellan R B 1996 *J. Phys. Chem. Solids* **57** 233
[17] Redhead P A 1962 *Vacuum* **12** 203
[18] Cerofolini G F and Re N 1995 *J. Colloid Interface Sci.* **178** 428
[19] Griffith R and Pryde J A 1967 *Trans. Faraday Soc.* **63** 2522
[20] Boszo F, Ertl G, Grunze M and Weiss M 1977 *Appl. Surf. Sci.* **1** 103
[21] Mundenar J M, Murphy R, Tsuei K D and Plummer E W 1988 *Chem. Phys. Lett.* **143** 593
[22] Gleason N R, Gerken C R and Strogin D R 1993 *Appl. Surf. Sci.* **72** 215
[23] Brzóka K D and Kleint C 1976 *Thin Solid Films* **34** 131
[24] Koel B E, Peebles D E and White J M 1983 *Surf. Sci.* **125** 709
[25] Richter L J, Gurney B A and Ho W 1987 *J. Chem. Phys.* **86** 477
[26] Yates J T and Madey T E 1971 *J. Chem. Phys.* **54** 4969
[27] Redhead P A, Hobson J P and Kornelsen E V 1993 *The Physical Basis of Ultrahigh Vacuum* (New York: American Vacuum Society) p 369
[28] Checchetto R, Gratton L M, Miotello A, Tomasi A and Scardi P 1998 *Phys. Rev.* B **58** 4130
[29] Buschow K H J, Bouten P C P and Miedema A R 1983 *Rep. Prog. Phys.* **45** 937
[30] Chen X Y and Wan X J 1998 *Scr. Mater.* **38** 1505
[31] Schwendemann B and Kronmueller H 1987 *Phil. Mag.* A **55** 683
[32] Moeller W and Roth J 1986 *Physics of Plasma–Wall Interactions in Controlled Fusion* ed D E Post and R Behrisch (New York: Plenum) p 439
[33] Myers S M, Besenbacher F and Norskov J K 1985 *J. Appl. Phys.* **58** 1841
[34] Besenbacher F, Myers S M, Nordlander P and Norskov J K 1987 *J. Appl. Phys.* **61** 1788
[35] Thomas G J 1981 *Hydrogen Effects in Metal* ed M Bernstein and A W Thompson (Warrendale, PA: TMS-AIME) p 77
[36] Au J J and Birnbaum H K 1978 *Acta Metall.* **26** 1105
[37] Edwards R A H and Eichenauer W 1980 *Scr. Metall.* **14** 971
[38] Mutschele T and Kirchheim R 1987 *Scr. Metall.* **21** 135
[39] Myers S M and Follstaedt D M 1988 *J. Appl. Phys.* **63** 1942
[40] Huang X Y, Mader W and Kirchheim R 1991 *Acta Metall.* **39** 893
[41] Pressouyre G M and Bernstein I M 1978 *Metall. Trans.* A **9** 1571
[42] Bogner J, Steiner W, Reissner M, Mohn P, Blaha P, Schwarz K, Krachler G, Ipser H and Sepiol B 1998 *Phys. Rev.* B **58** 14 922
[43] Schaefer E H, Damson B, Weller M, Arzt E and George E P 1997 *Phys. Status Solidi* a **160** 531
[44] Myers S M, Picraux S T and Stoltz R E 1980 *Appl. Phys. Lett.* **37** 168
[45] Würschum R, Grupp C and Schaefer H E 1995 *Phys. Rev. Lett.* **75** 97

[46] Checchetto R, Miotello A and Tomasi A 1999 *Chem. Phys. Lett.* **306** 330
[47] Campone P, Spinolo G, Vedda A, Checchetto R, Gratton L M, Miotello A and Tomasi A 1996 *Solid State Commun.* **98** 917
[48] Martin J J 1988 *IEEE Trans. Ultrason. Ferroelectr. Control* **35** 288
[49] Checchetto R, Gratton L M and Miotello A 2001 *Surf. Coat. Tech.* at press
[50] Bayer W and Wagner H 1981 *Solid State Commun.* **39** 375
[51] Lide D R (ed) 1977 *CRC Handbook of Chemistry and Physics* (West Palm Beach, FL: Chemical Rubber Company Press)
[52] Fanciulli M, Zenkovich A and Weyer G 1998 *Appl. Surf. Sci.* **124** 207